

Research Article

From Geophysics to Microgeophysics for Engineering and Cultural Heritage

P. L. Cosentino, P. Capizzi, R. Martorana, P. Messina, and S. Schiavone

Dipartimento delle Scienze della Terra e del Mare, University of Palermo, 90123 Palermo, Italy

Correspondence should be addressed to P. L. Cosentino, pietro.cosentino@unipa.it

Received 16 February 2011; Accepted 25 March 2011

Academic Editor: Francesco Soldovieri

Copyright © 2011 P. L. Cosentino et al. This is an open access article distributed under the Creative Commons Attribution License, which permits unrestricted use, distribution, and reproduction in any medium, provided the original work is properly cited.

The methodologies of microgeophysics have been derived from the geophysical ones, for the sake of solving specific diagnostic and/or monitoring problems regarding civil engineering and cultural heritage studies. Generally, the investigations are carried out using different 2D and 3D tomographic approaches as well as different energy sources: sonic and ultrasonic waves, electromagnetic (inductive and impulsive) sources, electric potential fields, and infrared emission. Many efforts have been made to modify instruments and procedures in order to improve the resolution of the surveys as well as to significantly reduce the time of the measurements without any loss of information. This last point has been achieved by using multichannel systems. Finally, some applications are presented, and the results seem to be very promising and promote this new branch of geophysics. Therefore, these methodologies can be used even more to diagnose, monitor, and safeguard not only engineering buildings and/or large structures, but also ancient monuments and cultural artifacts, such as pottery, statues, and so forth.

1. Introduction

Microgeophysics is one of most recent branches of geophysics. It includes a lot of methodologies derived from geophysics and it is applied, with more or less miniaturized instrumentations, to small volumes of soil or masonry, as well as to simple artifacts such as statues, pottery, corbels, and so forth.

At the beginnings of the 90s, little by little microgeophysics was born following the miniaturization of geophysical instrumentation, in particular transducers both transmitter and receivers, so that they could be adapted to small-scale and very small-scale applications.

Indeed, the very first attempts of miniaturization were carried out in the 1950s, when many researchers were used to build physical models on a small scale (e.g., [1–3]) to evaluate the possibilities offered by some new geophysical methods or to test the results obtained by the standard methodologies on particular not simple soil models [4]. In fact, at that time personal computers had still not been developed, so a lot of the problems encountered in the field of applied geophysics were simply solved by using physical

models on a small scale rather than mathematical models. Such physical models were often built in appropriate tanks using various kind of materials (see, for instance, [5]), either natural or not. In some rare cases, the models were made in small pieces of subsoil suitably prepared. But, these kinds of studies did not allow researchers to obtain models with high-resolution details, thereby necessitating a great deal of additional investigation over the years. However, this in turn contributed to the advancement of the investigation and physical tests on small structures and objects, certainly promoting the birth of this new branch of geophysics.

Furthermore, the advent of digitalization and the development of effective a/d converters stimulated both the simultaneous sampling of a large number of channels (i.e., the manufacture of multichannel instruments) and speeding up processing and interpretation of the acquired data by means of computers driven by appropriate software programs.

However, microgeophysics is an expanding branch: major demands come from conservation and restoration in the fields of civil engineering and management of ancient monuments and cultural heritage artifacts, the science of materials being also a growing source of incentives and

suggestions. This is especially true as far as works of art are concerned, where the choice of methodology has been greatly influenced by the noninvasive characteristics of the methodologies of microgeophysics. In fact, microscopic methodologies that damage very small volumes provide a lot of information, but may turn out not to be representative of large volumes of the investigated artifact, whereas geotechnical macroscopic methodologies involving large volumes are generally more or less destructive.

As a matter of fact, over the last 30 years many different types of investigation have been implemented, often derived from other fields of study, for instance, the electrical resistivity tomography for stone columns, which in turn derives from medical diagnostics.

Microgeophysics noninvasive methods can be used in situ and are characterized by an resolution power that can be defined between “microscopic” and “macroscopic” investigations, ranging from a few centimeters to a few decimeters: such a resolution can be very useful for artifacts having dimensions from a few cubic decimeters to a few cubic meters. Therefore, the miniaturization of the methods of applied geophysics can well cover these kinds of small-sized targets (artifacts, columns, pillars, pottery, statues, museum objects, etc.), provided that investigations are integrated with other specific methodologies to evaluate particular physical and chemical aspects, sometimes also including the biological ones.

Even though there are not yet basic key papers on Microgeophysics but only papers regarding particular methodologies and/or case histories (some of them are included in the reference list), the involved methodologies are often applied to structures of civil engineering, ancient monuments, and cultural heritage items. The word “geo” is still present even though the investigated targets are not only sculptured rocks, but also include metallic, vitreous, ceramic, and even wooden artifacts. The main peculiarity of these investigations, compared with those of classical applied geophysics, is that the objects to be inspected generally offer more than one face, which can be looked into by injecting the necessary energy and by positioning the required external and/or internal probes in every point of the object. Therefore, they generally give better results if compared with those offered by classical geophysical investigations, which lose in resolution when the investigated depth increases.

2. Technical Problems

One of the main technical problems encountered by microgeophysics is related to the miniaturization of all the transducers, both transmitters and receivers. Obviously, there are some important differences regarding the methodology to be used, that is, potential fields (principally the electric fields) or wave fields, either mechanical or electromagnetic.

A normal assumption of geophysics is that both, transmitters and receivers, are punctiform with respect to the geometrical parameters of the model used. As in microgeophysics the models are undoubtedly small-sized with respect to those of geophysics, it is still harder to consider punctiform



FIGURE 1: Sandbags on the ECG electrodes (used only for potential measures) on the floor of the Ambulatory of the great hunt at the “Villa del Casale,” Piazza Armerina [30].

normal geophysical sources and probes, like geophones, hammers, steel pegs, GPR antennas, and so forth.

The problem has been faced in many ways, and different solutions have been studied to replace sources and probes with other small-sized ones.

The steel pegs having a length of 40–60 cm, normally used for geoelectrical survey, have been replaced by small steel nails (6–8 cm in length, 1.5–2 mm in diameter) and, where it is possible, by disposable electrocardiogram (ECG) electrodes (with a diameter of about 1 cm but with no extension in penetration inside the artifact) provided with external adhesive strips. The inconveniences of the ECG electrodes are two: (1) if they have to be put in roughly vertical or upside down positions (i.e., walls, columns, ceilings, etc.) the adhesion to the artifact is very critical or impossible, depending on the conditions of the surface of the artifact and (2) the contact resistance is rather high (higher than few $M\Omega$) and it is generally changing in time during some hours, that is the time that generally is necessary to place them on the wall—or floor or body—to be studied. This time can be up to 100 to 150 min, depending upon the number of electrodes and the type of object being studied. The final typical values of contact impedances range from 0.1 to 100 $M\Omega$ depending on the investigated lithotype and the treatment of its exposed surface. Obviously, these high contact impedances have to be suitably reduced in the current electrodes in order to inject an appropriate current intensity.

A lot of enterprises around the world produce these kinds of electrodes, but of the ones we tested the best we selected are those in Foam Ag/AgCl (adult-type F 9047 manufactured by FIAB). The main advantage of these electrodes consists in the relative time stability of their contact resistance: in fact, it is very important that the contact resistances remain more or less stable for the period of positioning all the set of electrodes in the artifact; otherwise, the electrodes would have contact resistance very different the one from the other, in such way inserting different errors in the electric potential measures. Unfortunately, large currents through these electrodes can burn them, so that it is sake to avoid to use them as current electrodes. Sometimes, when they have to be put on the floor (or on a horizontal surface), the adhesive stripes can be removed and a sandbag can be used as a weight to assure the contact (Figure 1). Alternatively, flat electrodes can be successfully used [6].

The geophones have been replaced by small or very small piezoelectric accelerometers, today very popular, which are



FIGURE 2: One transmitter and two ultrasonic receivers on the statue of Togato di Petrarà (2nd century A.D.) [31].



FIGURE 3: Transmitting and receiving GPR antennas (IDS, 1600 MHz) on the statue of S. Michele Arcangelo (Gagini's apprentices, 1530-50), at the Museum Abatellis, Palermo Italy [32].

also contained in many smartphones. Typical accelerometers have a shape similar to a thin drop with diameter about 1 cm, so that the correct positioning in microgeophysical survey can be considered reliable enough. The ones we selected for quality-to-price ratio are manufactured by Japanese Murata & Co (namely, type 6CC-10-3R9-1000). They have been successfully tested and used in many professional and research works. However, many other piezoelectric seismometers are manufactured around the world and are available on the world market (e.g., Kistler, STMicroelectronics, SensComp, etc.).

Generally, ultrasonic transducers (both, transmitters and receivers) are rather large (diameter about 3–6 cm, height about 4–8 cm). For microgeophysics surveys, it is a good rule to use cone-shaped extensions in order to considerably reduce the contact surface so improving the precision of the positioning (Figure 2).

As far as the GPR probes concerned, we can say that it is still a problem to handle the probes for microgeophysical surveys. In fact, the antennas manufactured and available are still too large, especially those which are in combined (transmitter-receiver) box (they are most of the commercial ones). Even those which are arranged in separated box (we use that manufactured by IDS, Italy, Figure 3) are rather large in size, because the boxes generally contain the electronics, too. However, the positioning of these antennas is more precise than the combined ones, where two dipoles are present.

Hopefully, in the future new separated antennas with an only shielded dipole connected by a semirigid cable with an easily handy box will be manufactured by Enterprises which will be heedful to this market segment.

Today, the multichannel instruments are being improved all over the world, increasing the sampling rate (higher sampling frequencies) and avoiding large multiplexing so to have a real simultaneous acquisition of all the channels. In particular, this should be made for microgeophysical instruments, for which the very short times to be measured impose larger and larger sampling rate.

3. Resolution

Resolution is one of the most important parameter of the tomographic approach. It should be faced very carefully, as it is primarily determined in the first phase of the survey, that is, the acquisition. In fact, the number and space density of the acquired data, both in potential field and in wave field tomography, are the main parameters can limit the maximum obtainable resolution.

It is important to remind the main differences of using energy sources given by potential fields, where geophysical responses are prevalently given by the investigated earth volumes, or by wave fields, where geophysical responses are prevalently given by the reflecting, refracting, and diffracting surfaces that separate different parts of the interior of the investigated artifacts. According to this important difference, body parameters are involved in the first case and surface-parameters are at stake in the second one. These differences heavily affect the tomographic approach, as the potential field tomography originates from an inversion of contributions given by volume units, while wave field tomography is based on the analysis and reconstruction of ray paths of the waves traveling into the investigated volume. However, in both cases tomography is carried out keeping a particular prearranged order among the places of the transmitting and receiving probes. Commonly, the number of transmitting and receiving probes is equal, leading to nearly-symmetrical arrangements. But sometimes the number of transmitting and receiving probes is different, especially in sonic and ultrasonic tomography, where transmitting and receiving probes are very alike and separated, so that for each ray they can be exchanged each other without any difference in the results.

In some cases, especially in ERT survey, places of transmitting and receiving probes are constrained by a particular kind of array which has been selected for acquisition. In particular, we would recommend the use of the MYG array [7] using a lot of receiving probes and few transmitting ones (without any precise geometrical constrain), especially for cases in which surfaces are vulnerable, then avoiding the employment of many nails because, although they are small, they can damage the surface.

When wave fields are concerned, another parameter can limit the resolution, that is, the frequency for the waves used, as in turn it is responsible of wave diffractions and consequent loss of energy. Therefore, higher resolution required by microgeophysics generally demands the use of higher frequencies, in spite of the smaller waves' penetration depth. A compromise, if possible, should be made between the increase in the resolution and the decrease in the penetration depth. On the contrary, if lower frequencies are

to be used to obtain a higher penetration depth, diffracted waves can be used to study small targets; however, the analysis of diffracted waves is complicated and represents an emerging field of microgeophysics.

However, the resolution attainable using a rich set of experimental data should be maintained with an appropriate inversion in order to obtain the final tomographic restitution both in a 2D or 3D model.

The preliminary choice of any inversion is the geometrical arrangement of the pixels (2D) or voxels (3D): it depends on many parameters and, primarily, on those already mentioned linked to the acquisition array. These parameters are essential in potential methods, like ERT, but they should be combined with the physical discriminating power of the used methodology.

In potential field methodologies this power is limited by the “distance” of the objects from the observation instruments (transmitters and receivers generally located on the surfaces), so that the distinguishable voxels (3D) or pixels (2D) should be larger and larger when the distance (depth) increases.

In wave field methodologies (sonic, ultrasonic, and GPR), the discriminating power is limited by the “frequency” of the waves arriving to the detecting probes (i.e., the used frequencies, as filtered by the investigated sample). The frequencies should be obviously transformed in wavelengths taking into account the velocity of the waves. The wavelength allows us to calculate the Fresnel zone radius and consequently the discriminating power (namely, the lateral resolution r) at various distances, following Cerveny and Soares [8], as

$$r = \left[L \frac{\lambda}{2} + \left(\frac{\lambda}{4} \right)^2 \right]^{1/2}, \quad (1)$$

where L being the ray length and λ the wavelength calculated using $\lambda = v/f$, v is the velocity of the wave, and f is the frequency.

In sonic survey, a pulse is generally used as energy source, and therefore its spectral content is practically very large (depending on the hammer used), going to very high frequencies. On the contrary, in both electromagnetic GPR and ultrasonic survey, a single frequency source is used: but, this frequency, which is also characteristic of the used transducer, is modulated by a squared shape pulse, producing a signal characterized by a large band. In this way in all the waves field methodologies we are able to send signals characterized by very high frequencies, which in turn will be subjected to the cruel attenuation law smoothing higher frequencies much more than the lower ones. However, we have to consider, when we keep the first arrival of the signals, the frequencies contained in the first rises of the arrivals, that is we have to look at the steep slope of the first arrivals. Our experience is that this part of the signals contains very high frequencies; anyhow, the maximum contained frequency of the signals decreases when the distances increase.

By the light of the above line of reasoning, in order to evaluate the lateral resolution we should use as frequency

f in (1) the maximum frequency retrieved in the picking of the first arrivals to the detecting probes, which are the real information sources in order to obtain a velocity tomography. Such maximum frequencies are generally much higher than the nonmodulated monochromatic frequency of the transmitter. However, these maximum frequencies also depend on the sampling rate, following the well known sampling rule given by the Nyquist-Shannon sampling theorem [9, 10].

4. Some Case Histories

A few cases histories regarding ERT, ultrasonic, and GPR tomography are reported in order to discuss the applications of such simple rules we presented in the previous paragraphs.

4.1. Electrical Resistivity Tomography. An example of “full-3D” electrical resistivity tomography carried out on a wall is here presented. The aim was to understand the cause of moisture on a wall of the fountain room of the Zisa Palace (Palermo, XII century A.D., Figure 4(a)), covered by a precious mosaic interested by an important detachment of tesserae (Figure 4(b)). Therefore, we placed a regular grid of 11×16 adhesive electrodes, covering an area of 2 m high and 3 m wide. In order to assure a very low impact on the mosaic structure, only 15 nails electrodes were used for the current injection, driven into very small holes (2 mm of diameter) drilled in the interstices among the mosaic tesserae.

For each current injection, 176 potential measurements were acquired simultaneously with the MRS256 instrument (GF Instruments), between each electrode of the acquiring grid and a reference electrode (for an amount of 38 different current dipoles). In this way, the set of 6688 experimental data is very flexible, so to allow any calculation of potential difference between any of the possible electrode couples of the grid.

Then, the apparent resistivity values were calculated selecting the potential dipoles as close as possible to the hypothetical current lines in the medium, using the Maximum Yield Grid methodology [7, 11]. 1769 data have been considered as outliers and 4919 data have been processed using Res3D inv software [12].

The geometrical model was made by ten layers with 6000 voxels (10×10 cm in each layer). The layer thicknesses increase with the depth from 0.05 m (1st layer) to about 0.12 m (10th layer) following the decrement of resolution with depth.

The resulting tomographic inverted model of resistivity distribution (Figure 4(c)) presents a large volume characterized by low resistivity values, that seems to be originated in the middle of the wall, in correspondence with the water-pipe of the fountain. The conductive anomaly has been interpreted (as successively confirmed by a direct inspection) as a accumulation point of water inside the masonry, now clogged towards the fountain. The deep high resistivity volumes surrounding the accumulation point could be explained by the difference between the two exposed sides of the wall: the internal surface is covered by the mosaic that

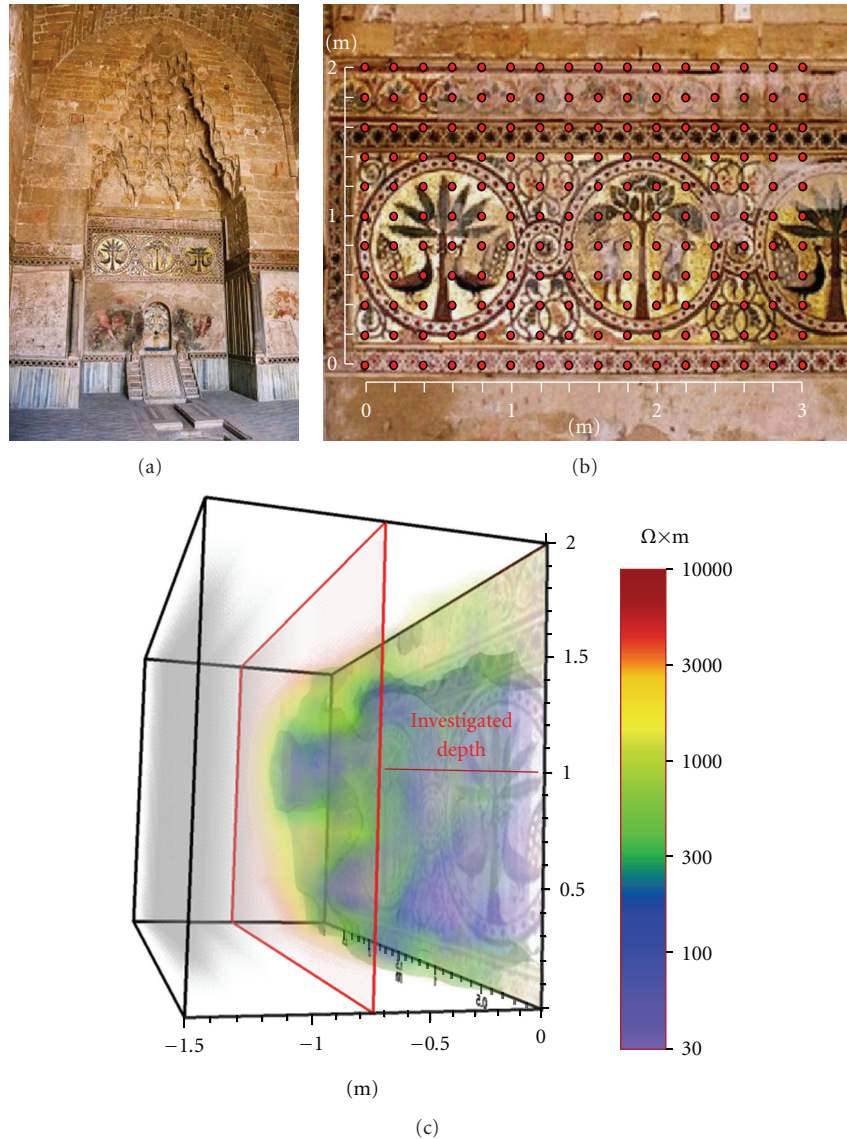


FIGURE 4: (a) Frontal wall of the Fountain Room of the Arabian Zisa Palace in Palermo; (b) part of the investigated mosaic wall where the grid of 176 potential electrodes was applied (red points). The 15 nails used to inject the current were inserted in as many selected points along the small, mortar-filled spaces between the tesserae of the mosaic; (c) 3D inversion model of the acquired data observed from the back of the wall (1.5 m thick). Due to the size of the grid used (2 m \times 3 m), the inversion model is limited to 0.75 m of depth. All dimensions are in meters (after [4], modified).

obstructs the moisture evaporation while the external one is not only mosaic free but also exposed to winds and sun (i.e., it is characterized by high drying capacity). It is evident how this substantially noninvasive investigation solved a serious restoration problem.

4.2. Ultrasonic Survey. Ultrasonic tomography for non-destructive tests and for characterization of artefacts has been applied in many case with good results [13–17]. In particular, 3D ultrasonic tomography has been recently used to study the structural continuity of the material [18–20].

We relate about the ultrasonic tomography carried out on the bust of Eleonora d’Aragona (sculptured by F. Laurana,

1468, Figure 5(a)), which is a beautiful work of art, finely carved from a block of white and microcrystalline marble. It is shown on the original support designed by the architect Carlo Scarpa in the 60s.

The cleanup of the sculpture has revealed a fracture that probably originated on a natural veining of the marble block in the central portion of the neck, involving the whole face of the lady. To better understand the nature of this feature, a 3D ultrasonic tomography, obtained from 157 measurement points identified along the surface of the work, was performed [21]. The measure points were spaced 2–5 cm, so that 1832 signals corresponding to as many paths were acquired using the TDAS 16 Boviar multichannel

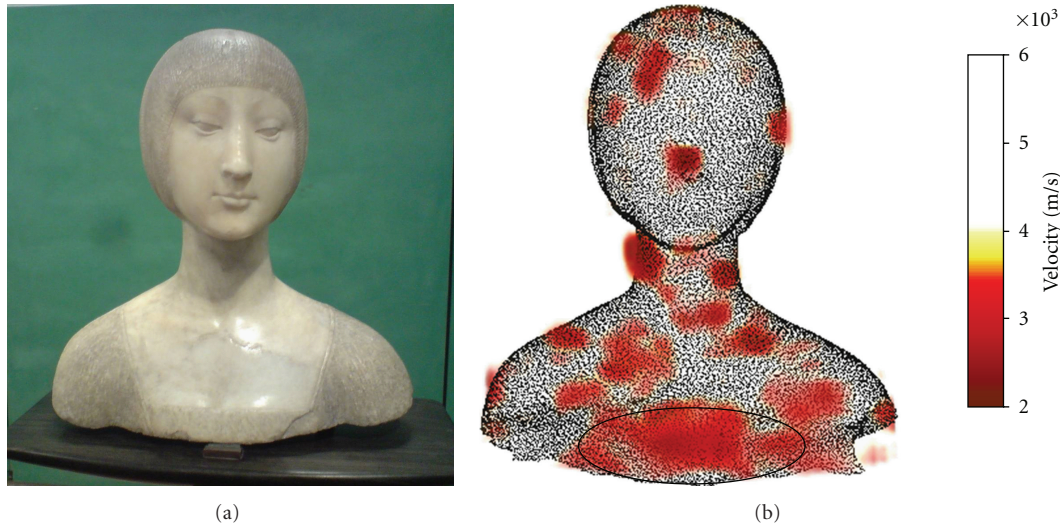


FIGURE 5: At left the bust of Eleonora d'Aragona (F. Laurana, 1468). At right the frontal 3D image with transparency of the investigated volume showing an area at low velocity, corresponding to the support point of the bust [21].

system, which acquires up to 16 channels using an electronic switch on four channels at a time with a maximum sampling rate of 1.25 MHz. The equipment is supplied with receiver and transmitter probes characterized by a central frequency of 55 kHz. 64 signals were discarded because considered outliers, while 1768 of these were processed. A comparison between results obtained using different cell dimensions were carried out and finally we decided to use a $1 \times 1 \times 1 \text{ cm}^3$ cell size for inversion process (Figure 5), performed with GeoTomCG software which performs inversions with the simultaneous iterative reconstruction technique (SIRT, [22]). Curved ray tracing was used with a revised form of ray bending, derived from the method given by Um and Thurber [23].

The model does not show significant discrepancies at the lesion on the face of the lady. Also the upper torso (head and neck) shows velocity values corresponding to a sufficiently homogeneous and well-preserved marble. However, the velocity model shows low values in the lower front portion of the trunk at the breast, according to the traveltime graph analysis.

This area bears the entire weight of the work; that is why the architect Carlo Scarpa designed the original support.

Even in this case, the noninvasive tomographic investigation solved a serious doubt raised by the restorers and our beautiful lady Eleonora continued travelling in the Museums all over the world.

4.3. GPR Surveys Integrated with Ultrasonic Tomography. The large size of the GPR antennas does not allow up to now a resolution similar to that of ultrasonic and ERT tomographies, especially when irregular surfaces are concerned. Therefore, GPR surveys are generally integrated with ultrasonic and/or electrical tomographies, substantially improving the obtained results. One of these cases is here discussed.

The archaeological Museum of Rome asked our group to inquire into the physical consistency of a marble slab (II-III century AD) that has recently fallen down during its travel for being part of an exhibition. We decided to use different methodologies to investigate the slab: namely, a pacometer (Protovale Elcometer) to individuate internal coupling pins, GPR (2000 MHz), and Ultrasonic (55 kHz) tomographic high-density surveys to investigate the internal extension of all the visible fractures and to search for the hidden ones.

4.3.1. Ultrasonic Tomography. The acquisition was realized using 65 measurement points, 40 distributed on the thickness of the slab side and 25 on the relief. The distance between two consecutive probe positions was set to 100 mm, for measurement points distributed on the external thickness of the slab side. Ultrasonic measures were carried out using the TDAS 16 Boviar multichannel system, which acquires up to 16 channels using an electronic switch on four channels at a time with a maximum sampling rate of 1.25 MHz. The equipment is supplied with receiver and transmitter probes characterized by a central frequency of 55 kHz.

A total of 961 signals were acquired and processed, on which the traveltimes of elastic waves were measured by picking procedures. Inversion process were carried out using $2 \times 2 \times 2 \text{ cm}^3$ cell size, with GeoTomCG software and curved ray tracing [23].

A total of 961 signals were acquired and processed, on which the traveltimes of elastic waves were measured by picking procedures.

The tomographic model (Figure 6) shows velocity values with a minimum of about 1500 m/s and a maximum of about 5000 m/s (that is probably the velocity of the original marble). This lack of homogeneity and the presence of low velocity values suggest that the state of the marble is poor, especially in correspondence of the injury of the slab

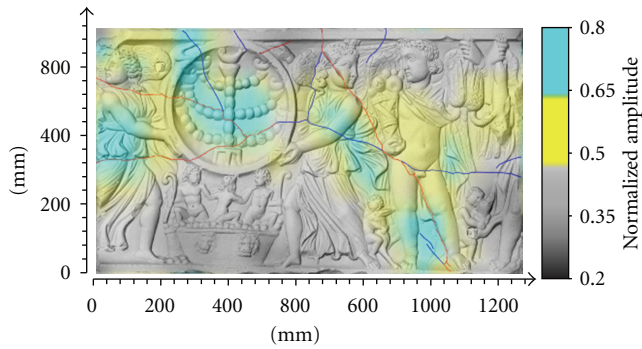


FIGURE 6: Smoothed 2D tomographic section, using $2 \times 2 \text{ cm}^2$ cell dimension, superimposed to slab image.

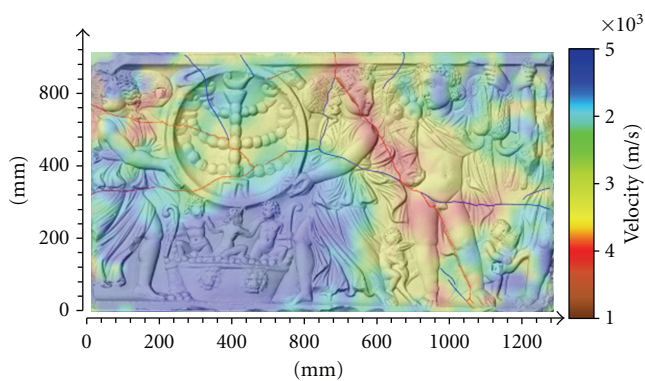


FIGURE 7: GPR tomography superimposed to slab image.

(recent or not) as evidenced by the superimposition of a tomographic ultrasonic image on the relief of the slab.

4.3.2. GPR Surveys. GPR method used to detect small discontinuities is not simple, but several studies have been carried out to locate subsurface fractures and all of them showed that GPR can give good results [17, 24–29].

GPR surveys to the roman marble slab were carried out using the Aladdin system (IDS), with a 2 GHz bipolar antenna. Considering the direction of the maximum elongation of the slab, 12 longitudinal and 7 transverse profiles were acquired. This configuration allowed us to obtain a good sampling of the data, achieving tomographic images with high detail.

GPR processed data were used to construct depthslices which were calculated with our procedure implemented in Matlab environment. The appropriate analysis window was chosen depending on the shape, size, and location of anomalies detected with ultrasonic surveys. In particular, we chose an analysis window of 0.25 ns along the time axis and 0.05 m along the distance axis. The depthslice presented in Figure 7 corresponds to the central depth of the slab. The scale of the amplitudes in the presented map was normalized to the maximum value recorded.

Even radar tomography shows a strong correlation with observable cracks in the slab, and therefore also with ultrasonic tomography. The detected anomalies correspond

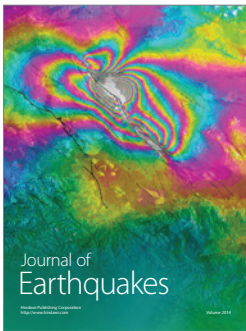
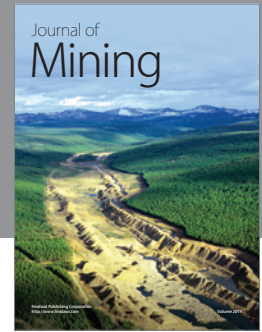
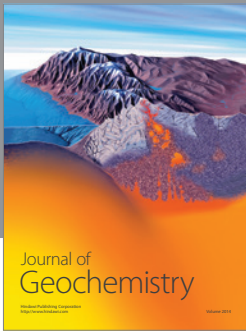
to changes in em properties of the material as well as to metallic elements of reinforcement.

As regards the results given to the Museum, we affirmed that the slab was in very bad condition, having reduced physical-mechanical characteristics. The falling of the marble slab caused a weakening of the marble and a deterioration of its mechanical properties: beside the existing lesions, the development of new lesions practically covered the whole slab. The damage caused to the material was not easily remediable because the characteristics of the material cannot be reconstructed before undergoing such a trauma. The restorers proceeded to plan a steel containment belt, with reversible support, in order to raise the slab and let the artwork be admired both from the front side and the back one. Successively, a suitable consolidation project has been planned to reinforce the whole marble structure.

References

- [1] A. Apparao, "Model tank experiments on resolution of resistivity anomalies obtained over buried conducting dykes—inline and broadside profiling," *Geophysical Prospecting*, vol. 27, no. 4, pp. 835–847, 1979.
- [2] A. Apparao, A. Roy, and K. Mallick, "Resistivity model experiments," *Geoexploration*, vol. 7, no. 1, pp. 45–54, 1969.
- [3] A. Apparao and A. Roy, "Resistivity model experiments-II," *Geoexploration*, vol. 9, no. 4, pp. 195–205, 1971.
- [4] P. L. Cosentino, P. Capizzi, G. Fiandaca, R. Martorana, and P. Messina, "Advances in microgeophysics for engineering and cultural heritage," *Journal of Earth Science*, vol. 20, no. 3, pp. 626–639, 2009.
- [5] W. Goudswaard, "On the effect of the tank wall material in geoelectrical model experiments," *Geophysical Prospecting*, vol. 5, no. 3, pp. 272–281, 1957.
- [6] E. N. Athanasiou, P. I. Tsourlos, G. N. Vargemezis, C. B. Papazachos, and G. N. Tsokas, "Non-destructive DC resistivity surveying using flat-base electrodes," *Near Surface Geophysics*, vol. 5, no. 4, pp. 263–272, 2007.
- [7] G. Fiandaca, R. Martorana, P. Messina, and P. L. Cosentino, "The MYG methodology to carry out 3D electrical resistivity tomography on media covered by vulnerable surfaces of artistic value," *Il Nuovo Cimento B*, vol. 125, no. 5-6, pp. 711–718, 2010.
- [8] V. Cerveny and J. E. P. Soares, "Fresnel volume ray tracing," *Geophysics*, vol. 57, no. 7, pp. 902–915, 1992.
- [9] U. Grenander, *Probability and Statistics, Harald Cramér Volume*, Almquist & Wiksell, 1959.
- [10] H. L. Stiltz, *Aerospace Telemetry*, Prentice-Hall, New York, NY, USA, 1961.
- [11] G. Fiandaca, R. Martorana, P. Messina, and P. L. Cosentino, "3D ERT for the study of an ancient wall covered by precious mosaics," in *Proceedings of the Near Surface 15th European Meeting of Environmental and Engineering Geophysics*, Dublin, Ireland, 2009.
- [12] M. H. Loke, "Tutorial : 2-D and 3-D electrical imaging surveys," 2010.
- [13] L. Binda, A. Saisi, C. Tiraboschi, S. Valle, C. Colla, and M. Forde, "Application of sonic and radar tests on the piers and walls of the Cathedral of Noto," *Construction and Building Materials*, vol. 17, no. 8, pp. 613–627, 2003.
- [14] J. Blitz and G. Simpson, *Ultrasonic Methods of Non-Destructive Testing*, vol. 2 of *Non-Destructive Evaluation Series*, 1996.

- [15] K. A. Dines and R. J. Lytle, "Computerized geophysical tomography," *Proceedings of IEEE*, vol. 67, no. 7, pp. 1065–1073, 1979.
- [16] W. S. Phillips and M. C. Fehler, "Traveltime tomography: a comparison of popular methods," *Geophysics*, vol. 56, no. 10, pp. 1639–1649, 1991.
- [17] L. Sambuelli, G. Bohm, P. Capizzi, E. Cardarelli, and P. Cosentino, "Comparison among GPR measurements and ultrasonic tomographies with different inversion algorithms. An application to the basement of an ancient Egyptian sculpture," *Journal of Geophysics and Engineering*, vol. 8, pp. 1–11, 2011.
- [18] P. Capizzi, P. Cosentino, and S. Schiavone, "Ultrasonic tomographic analysis for getting information on the mechanical structure of ceramic tiles," *Environmental Semeiotics*, vol. 2, no. 2, pp. 110–119, 2009.
- [19] P. Capizzi, P. L. Cosentino, A. Danesi, G. Fiandaca, and S. Gambardella, "Indagini fisiche a supporto dell'intervento di restauro di una lastra marmorea del II-III d.C. Atti del," in *VII Congresso Nazionale IGHC—Lo Stato dell'Arte 7*, pp. 457–462, Napoli, Italy, October 2009.
- [20] E. Cardarelli and R. de Nardis, "Seismic refraction, isotropic anisotropic seismic tomography on an ancient monument (Antonino and Faustina temple AD 141)," *Geophysical Prospecting*, vol. 49, no. 2, pp. 228–240, 2001.
- [21] F. Agnello, M. Cannella, P. Capizzi, P. Cosentino, L. Pellegrino, and S. Schiavone, "Indagini 3D di dettaglio per l'analisi dell'integrità del busto di Eleonora d'Aragona (F. Laurana, 1468)," *Atti del 28° Convegno GNGTS*, vol. 28, 521–523, Novembre 2009.
- [22] J. E. Peterson, B. N. P. Paulsson, and T. V. McEvelly, "Applications of algebraic reconstruction techniques to crosshole seismic data," *Geophysics*, vol. 50, no. 10, pp. 1566–1580, 1985.
- [23] J. Um and C. Thurber, "A fast algorithm for two-point seismic ray tracing," *Bulletin of the Seismological Society of America*, vol. 77, no. 3, pp. 972–986, 1987.
- [24] M. Bavusi, F. Soldovieri, S. Piscitelli, A. Loperte, F. Vallianatos, and P. Soupios, "Ground-penetrating radar and microwave tomography to evaluate the crack and joint geometry in historical buildings: some examples from Chania, Crete, Greece," *Near Surface Geophysics*, vol. 8, no. 5, pp. 377–387, 2010.
- [25] P. Capizzi and P. L. Casentino, "GPR multi-component data analysis," *Near Surface Geophysics*, vol. 6, no. 2, pp. 87–95, 2008.
- [26] G. Grandjean and J. C. Gourry, "GPR data processing for 3D fracture mapping in a marble quarry (Thassos, Greece)," *Journal of Applied Geophysics*, vol. 36, no. 1, pp. 19–30, 1996.
- [27] V. Pérez-Gracia, O. Caselles, J. Clapés, R. Osorio, J. A. Canas, and L. G. Pujades, "Radar exploration applied to historical buildings: a case study of the Marques de Llió palace, in Barcelona (Spain)," *Engineering Failure Analysis*, vol. 16, no. 4, pp. 1039–1050, 2009.
- [28] S. J. Radzevicius, E. D. Guy, and J. J. Daniels, "Pitfalls in GPR data interpretation: differentiating stratigraphy and buried objects from periodic antenna and target effects," *Geophysical Research Letters*, vol. 27, no. 20, pp. 3393–3396, 2000.
- [29] M. Rashed, D. Kawamura, H. Nemoto, T. Miyata, and K. Nakagawa, "Ground penetrating radar investigations across the Uemachi fault, Osaka, Japan," *Journal of Applied Geophysics*, vol. 53, no. 2-3, pp. 63–75, 2003.
- [30] P. L. Cosentino, P. Capizzi, G. Fiandaca et al., "Diagnostica per il consolidamento del mosaico pavimentale dell'ambulacro nella Villa Romana del Casale (Piazza Armerina)," in *XXIII Convegno internazionale—IL Consolidamento Degli Apparati Architettonici E Decorativi: Conoscenze, Orientamenti, Esperienze*, pp. 91–98, Bressanone, Italy, July 2007.
- [31] S. Gambardella, A. Danesi, P. L. Cosentino, P. Capizzi, and G. Fiandaca, "L'indagine sonica ed ultrasonica come prassi necessaria alla conoscenza di strutture complesse. Il rimontaggio di una statua di epoca romana da Locri: un caso esemplare," in *Atti del VI Congresso Nazionale IGHC—Lo Stato dell'Arte*, pp. 689–694, Spoleto, Italy, October 2008.
- [32] P. Capizzi, P. L. Cosentino, G. Fiandaca, R. Martorana, P. Messina, and I. Razo Amoroz, "Misure microgeofisiche sulla Statua del S. Michele Arcangelo (Scuola Gaginiana, XVI Sec.)," in *V Congresso Nazionale IGHC Lo Stato dell'Arte*, pp. 317–324, Cremona, Italy, October 2007.



Hindawi

Submit your manuscripts at
<http://www.hindawi.com>

